Prediction of progression of hepatic metastases from uveal melanoma using gadoxetic acid-enhanced magnetic resonance imaging

Ji Eun Lee[a], Sunyoung Lee[b], Jeong Ah Hwang[c], Seo-Youn Choi[c] and Ji Eun Moon[d]

MRI is the preferred method for evaluating hepatic metastases from uveal melanoma. This study was aimed to predict the progression of hepatic metastases from uveal melanoma using gadoxetic acid-enhanced MRI findings. This retrospective study included patients (≥18 years) with uveal melanoma who underwent gadoxetic acid-enhanced liver MRI for evaluation of hepatic metastasis between 2010 and 2023 at two tertiary referral centers. Radiologists retrospectively evaluated the baseline MRI findings of the included patients and assessed tumor responses on follow-up studies according to the Response Evaluation Criteria in Solid Tumors version 1.1. Independent prognostic factors for the time to progression of hepatic metastases were identified using Cox proportional regression analysis. A nomogram based on the multivariable analysis was created and internally validated. A total of 65 patients (mean age, 61.5 ± 14.0 years; 36 men and 29 women) were included. Multivariable analysis revealed that the size of the largest tumor [hazard ratio (HR): 1.028, $P = 0.005$], precontrast T1 hypointensity (HR: 3.033, $P = 0.016$), mild to moderate T2 hyperintensity (HR: 3.680, $P = 0.001$), and hepatobiliary phase hypointensity (HR: 3.370, $P = 0.020$) were significantly associated with shorter time to progressions of hepatic metastases from uveal melanoma. An internally validated nomogram developed using these MRI findings demonstrated excellent agreement between the predicted probabilities and actual rates of tumor progression, as shown by the calibration plots, with a Harrell's c-index of 0.807. Gadoxetic acid-enhanced MRI findings may be useful in predicting the progression of hepatic metastases from uveal melanoma. *Melanoma Res* **36: 211–218**

Melanoma Research 2026, **36**:211–218

Keywords: hepatic metastasis, magnetic resonance imaging, prognosis, uveal melanoma

[a]Department of Radiology, Soonchunhyang University College of Medicine, Bucheon Hospital, Gyeonggi-do, [b]Department of Radiology and Research Institute of Radiological Science, Severance Hospital, Yonsei University College of Medicine, [c]Department of Radiology and Center for Imaging Science, Samsung Medical Center, Sungkyunkwan University School of Medicine, Gangnam-gu, Seoul and [d]Department of Biostatistics, Clinical Trial Center, Soonchunhyang University College of Medicine, Bucheon Hospital, Gyeonggi-do, Republic of Korea

Correspondence to Sunyoung Lee, MD, PhD, Department of Radiology and Research Institute of Radiological Science, Severance Hospital, Yonsei University College of Medicine, 50-1 Yonsei-ro, Seodaemun-gu, Seoul 03722, Republic of Korea
Tel: +82 2 2228 7400; fax: +82 2 2227 8337; e-mail: carnival0126@gmail.com

Received 24 September 2025 **Accepted** 28 February 2026.

Introduction

With an incidence of 5.1 per million over the past 30 years, uveal melanoma is the most common primary intraocular malignancy among adults in the USA [1]. Cutaneous melanoma arises from melanocytes located in the basal layer of the epidermis, whereas uveal melanoma arises from melanocytes located in the uveal tract [2]. Approximately 85–90% of uveal melanomas are found in the choroid, while the rest are found in the iris or ciliary body [1,3]. Cutaneous and uveal melanomas are biologically distinct, differing in incidence and clinical behavior [2]. Uveal melanoma, in particular, has a strong tendency to metastasize to the liver, and shows a limited response to immunotherapy [4].

At present, the primary treatments for uveal melanoma include enucleation, radiotherapy, brachytherapy, and proton therapy [5,6]. At the time of diagnosis, less than 5% of patients have detectable metastases [7,8]. However, despite successful local treatment of the primary tumor, up to half of all patients with uveal melanoma develop metastasis, with the liver being the first and only site of metastasis in most patients [5,7]. The prognosis of patients with metastatic uveal melanoma depends largely on the presence and progression of hepatic metastasis [8].

Among the various imaging modalities, MRI is the preferred method for evaluating hepatic metastases from uveal melanoma [9], and can even accurately identify early hepatic metastases [10]. Melanin deposits in tumors cause shortening of T1 and T2 relaxation times,

Supplemental Digital Content is available for this article. Direct URL citations appear in the printed text and are provided in the HTML and PDF versions of this article on the journal's website, www.melanomaresearch.com.

resulting in a characteristically high signal intensity on precontrast T1-weighted image (T1WI) [9]. Although not specific to patients with uveal melanoma, Lee *et al.* [11] reported that positive enhancement on subtraction images and intermediate high signal intensity on T2WI were significantly associated with a higher risk of progression of hepatic metastases from melanoma. Mariani *et al.* [12] reported a nomogram for predicting the survival of patients with hepatic metastases from uveal melanoma based on liver MRI; however, they only focused on the number and size of the metastases. To the best of our knowledge, no previous study has evaluated the effects of different tumor signal intensities on various sequences of gadoxetic acid-enhanced liver MRI or how these signal intensities may reflect the progression of hepatic metastases from uveal melanoma. Therefore, the purpose of this study was to investigate potential predictors of the progression of hepatic metastases from uveal melanoma on gadoxetic acid-enhanced MRI and to utilize these findings to develop a predictive nomogram.

Methods

This retrospective study was conducted at two tertiary referral centers (Severance Hospital and Soonchunhyang University Bucheon Hospital, Republic of Korea). The institutional review boards approved the protocol for this study, and the requirement for written informed consent was waived, due to the retrospective nature of the study.

Study population

We searched the electronic databases to identify patients with uveal melanoma who underwent enucleation between January 2010 and December 2023. The inclusion criteria were patients (≥18 years) who underwent gadoxetic acid-enhanced liver MRI for evaluation of hepatic metastasis. The exclusion criteria were as follows: (a) no documented diagnosis of hepatic metastases in the liver MRI report (n = 174); (b) no liver MRI to evaluate imaging findings prior to treatment for hepatic metastases (n = 8); (c) surgical resection for a single hepatic metastasis (n = 12); (d) the presence of distant metastases other than hepatic metastases (n = 3); and (e) no follow-up contrast-enhanced abdominal computed tomography or liver MRI to assess the progression of the hepatic metastases (n = 8). Finally, a total of 65 patients with hepatic metastases from uveal melanoma were included in this analysis. A flow chart of the study population is shown in Fig. 1.

Magnetic resonance imaging examinations

All MRI examinations were performed using one of the following 1.5 or 3-T MRI system: Magnetom Avanto or Skyra (Siemens Healthineers, Erlangen, Germany), Intera Achieva (Philips Healthcare, Best, The Netherlands), or Discovery MR 750w or Signa HDxt (GE Healthcare, Chicago, Illinois, USA). The sequences obtained included single- or multishot T2WI, T1-weighted dual gradient-echo imaging (in- and opposed-phase), T1-weighted three-dimensional gradient-echo imaging with dynamic contrast enhancement, and diffusion-weighted imaging. T1-weighted sequences were obtained before and after the intravenous injection of gadoxetic acid (Primovist, Bayer Healthcare, Berlin, Germany) at a rate of 1.0 ml/s

Fig. 1

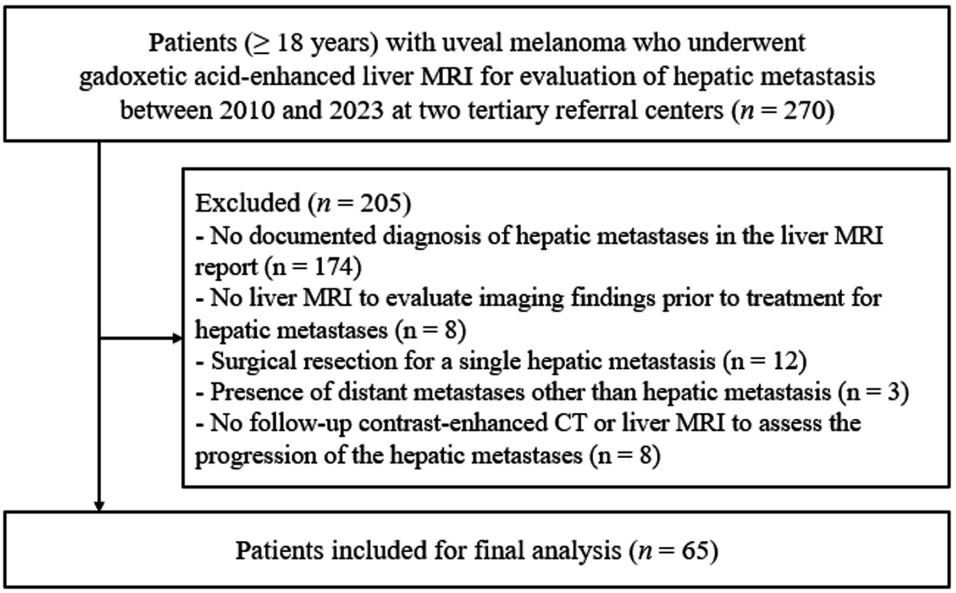

Flowchart of the study population.

(0.025 mmol/kg body weight). The test-bolus or bolus-tracking method was used to initiate arterial phase scanning, after which portal venous phase (60 s) and delayed phase (3 min) images were also obtained. Hepatobiliary phase images were obtained 15–20 min after the injection of the contrast agent. Subtraction images were obtained automatically by subtracting the unenhanced series from the arterial phase images. Further details of the MRI sequence parameters are presented in Table S1, Supplemental Digital Content, *https://links.lww.com/MR/A454*.

Clinical data collection

We retrospectively collected patients' clinical data from electronic medical records, including demographic characteristics and treatment methods for hepatic metastases from uveal melanoma. Treatments utilized included radiation therapy, transarterial chemoembolization (TACE), transarterial radioembolization, chemotherapy, or immunotherapy, as determined by the clinicians on an individual basis.

Magnetic resonance imaging analysis

A radiologist (J.A.H., with 13 years of experience in abdominal imaging) reviewed all gadoxetic acid-enhanced liver MRI and selected the target lesions for evaluation in each patient using a picture archiving and communication system. In cases of multiple hepatic metastases, the largest lesion was selected for MRI finding evaluation, while the two largest lesions were selected for tumor response evaluation. The diameters of the target lesions were also measured.

Two board-certified gastrointestinal radiologists (J.E.L. and S.L., both with 13 years of experience in abdominal MRI) independently reviewed the imaging data, except for the tumor size. The reviewers were aware that the hepatic lesions on MRI were metastases from uveal melanoma, although they were blinded to the clinical outcomes of patients.

The following image parameters were evaluated on the baseline gadoxetic acid-enhanced liver MRI: tumor signal intensity on: (a) precontrast T1WI (hyper- or isointensity vs. hypointensity); (b) T2WI (hypo- or isointensity vs. mild to moderate hyperintensity); (c) subtraction arterial phase images (isointensity vs. hyperintensity); or (d) hepatobiliary phase images (hyper- or isointensity vs. hypointensity); and (e) the presence of diffusion restriction, defined as higher signal intensity on diffusion-weighted imaging ($b = 800\,s/mm^2$) and lower signal intensity on apparent diffusion coefficient maps compared to the adjacent normal liver parenchyma. After each reviewer independently interpreted the images, any discrepancies were resolved by consensus discussion with a third reviewer (S.C., with 15 years of experience in abdominal imaging).

Evaluation of progression of hepatic metastases

All patients underwent follow-up contrast-enhanced abdominal computed tomography or liver MRI every 2–6 months. Tumor progression was defined as either more than 20% increase in the sum of the diameter(s) of the target lesion(s) or the development of one or more new lesions [13]. The presence or absence of hepatic metastasis progression was evaluated by a radiologist (J.A.H.) until the development of progression or until the last available scan through May 2024. Based on the tumor response, patients were categorized into either progression or nonprogression groups.

Statistical analysis

All statistical analyses were conducted using R version 3.6.0 (The R Foundation for Statistical Computing, Vienna, Austria) and Rex version 3.0.3 (RexSoft Inc., Seoul, Republic of Korea). To compare MRI findings between the progression and nonprogression groups, the two-sample t-test was used for continuous variables, and the chi-square or Fisher's exact test was used for categorical variables. Interobserver agreement between the two reviewers was assessed using the kappa (κ) statistic with the following interpretations: poor, less than 0.20; fair, 0.21–0.40; moderate, 0.41–0.60; good, 0.61–0.80; and excellent, 0.81–1.00.

Cox proportional regression analyses were performed on the consensus data to identify the gadoxetic acid-enhanced MRI findings associated with the time to progression (TTP) of hepatic metastases from uveal melanoma. Variables with a *P*-value less than 0.05 in the univariable analysis were further assessed in the multivariable analysis. We developed a nomogram to predict the probability of no progression at 3, 6, and 9 months and 1 year, using variables that identified significant independent predictors. Nomogram accuracy was evaluated using Harrell's c-index and calibration plots, where a c-index of 0.5 indicated random chance, 0.7 or higher indicated excellent consistency, and 1.0 indicated perfect predictive accuracy.

Results

Clinical and baseline magnetic resonance imaging data

The clinical and baseline MRI characteristics of the patients are shown in Table 1. A total of 65 patients with hepatic metastases from uveal melanoma were included in our analysis with a mean age of 61.5 ± 14.0 years (range, 28–84 years), of whom 36 (55.4%) were men and 29 (44.6%) were women. The mean size of the largest tumor on baseline liver MRI was 17.6 ± 18.6 mm. The tumor signal intensity showed hyper- or isointensity on precontrast T1WI in 87.7% (57/65), mild to moderate hyperintensity on T2WI in 52.3% (34/65), hyperintensity on subtraction arterial phase images in 50.8% (33/65), and hypointensity on hepatobiliary phase images in 64.6% (42/65) of the patients. Additionally, 60.0% (39/65) of the patients exhibited diffusion restriction of the tumor.

Treatments for hepatic metastases from uveal melanoma included radiation therapy ($n = 18$, 27.7%), TACE or transarterial radioembolization ($n = 4$, 6.2%), chemotherapy ($n = 40$, 61.5%), and immunotherapy ($n = 37$, 56.9%). Among the 65 patients, 34 (52.3%) received multiple treatment modalities for hepatic metastases, while 12 (18.5%) did not receive any treatment.

Interobserver agreement

Among the tumor imaging findings on MRI, signal intensity on T2WI exhibited excellent interobserver agreement, with a κ value of 0.845. Other imaging findings showed good interobserver agreement (κ = 0.685–0.747), except for tumor signal on subtraction arterial phase images (κ = 0.476), which only exhibited moderate interobserver agreement (Table S2, Supplemental Digital Content, *https://links.lww.com/MR/A454*).

Magnetic resonance imaging findings according to the progression of hepatic metastases

The MRI findings of the progression and nonprogressive groups are summarized in Table 2. The largest tumor size on baseline MRI was significantly larger in the progression group than in the nonprogression group ($P < 0.001$). The progression group also exhibited a significantly higher proportion of tumors with hypointensity on precontrast T1WI ($P = 0.046$), mild to moderate hyperintensity on T2WI ($P < 0.001$), hyperintensity on subtraction arterial phase images ($P = 0.001$), and hypointensity on hepatobiliary phase images ($P < 0.001$) than those in the nonprogression group. Additionally, tumors in the progression group were more likely to have diffusion restriction ($P < 0.001$).

Table 1 Clinical and baseline MRI characteristics of the study population

Characteristics	Number ($n = 65$)
Age (years)[a]	61.5 ± 14.0
Sex	
Male	36 (55.4)
Female	29 (44.6)
Baseline MRI characteristics	
Size of the largest tumor (mm)[a]	17.6 ± 18.6
Tumor signal intensity on MRI	
Precontrast T1WI	
Hyper- or isointensity	57 (87.7)
Hypointensity	8 (12.3)
T2WI	
Hypo- or isointensity	31 (47.7)
Mild to moderate hyperintensity	34 (52.3)
Subtraction arterial phase	
Isointensity	32 (49.2)
Hyperintensity	33 (50.8)
Hepatobiliary phase	
Hyper- or isointensity	23 (35.4)
Hypointensity	42 (64.6)
Diffusion restriction	
Absence	26 (40.0)
Presence	39 (60.0)
Treatment for hepatic metastasis[b]	
Radiation therapy	18 (27.7)
TACE or TARE	4 (6.2)
Chemotherapy	40 (61.5)
Immunotherapy	37 (56.9)
None	12 (18.5)

Unless otherwise stated, data are numbers of lesions with percentages.
MRI, magnetic resonance imaging; TACE, transarterial chemoembolization; TARE, transarterial radioembolization; T1WI, T1-weighted image; T2WI, T2-weighted image.
[a]Data are mean ± SD.
[b]Thirty-four patients received multiple treatment modalities for hepatic metastases.

Prognostic factors for predicting time to progression of hepatic metastases

In the multivariable analysis, the size of the largest tumor [hazard ratio (HR): 1.028, 95% confidence interval (CI): 1.008–1.048, $P = 0.005$], hypointensity on precontrast T1WI (HR: 3.033, 95% CI: 1.235–7.450, $P = 0.016$), mild to moderate hyperintensity on T2WI (HR: 3.680, 95% CI: 1.645–8.186, $P = 0.001$), and hypointensity on hepatobiliary phase images (HR: 3.370, 95% CI: 1.208–9.400, $P = 0.020$) were identified as significant independent variables that were associated with shorter TTP in patients with hepatic metastases from uveal melanoma (Table 3 and Table S3, Supplemental Digital Content, *https://links.lww.com/MR/A454*).

Prognostic nomogram based on magnetic resonance imaging findings

Using the significant independent baseline MRI variables identified in the multivariable analysis, we developed a prognostic nomogram to estimate the individual probability of no tumor progression at 3, 6, and 9 months and 1 year (Fig. 2) and generated calibration plots (Figure S1, Supplemental Digital Content, *https://links.lww.com/MR/A454*). The topmost scale, labeled "points" represents the contributions of each variable to the HRs. Among these variables, mild to moderate hyperintensity of the tumor on T2WI had the greatest impact on predicting TTP of hepatic metastasis from uveal melanoma. The total points for each patient were calculated as the sum of the individual variable points, and a perpendicular line was drawn below to determine the probability of no tumor progression at 3, 6, and 9 months and 1 year after the baseline MRI (Figs. 3 and 4). The estimated Harrell's c-index of the nomogram was 0.807, indicating excellent predictive accuracy and strong agreement between the predicted and observed TTP probabilities.

Discussion

Patient prognosis is strongly influenced by disease progression within the liver when uveal melanoma metastasizes to the liver [14,15]. In this study, we identified four gadoxetic acid-enhanced MRI findings that serve as independent predictors of TTP in patients with hepatic metastases from uveal melanoma, including the size of the largest tumor, precontrast T1 hypointensity, mild to moderate T2 hyperintensity, and hepatobiliary phase hypointensity of the tumor. Furthermore, the nomogram constructed using these imaging findings

demonstrated excellent concordance between the predicted and actual probabilities, as evidenced by the calibration plot.

Mariani *et al.* [12] reported that the size of the largest hepatic metastasis was significantly associated with overall survival in patients with uveal melanoma. Similarly, the result of our study showed a significant difference in the size of the largest hepatic metastasis on baseline MRI between the progression and nonprogression groups. Additionally, the size of the largest tumor identified a significant predictor of TTP for hepatic metastases from uveal melanoma. Therefore, larger tumor size and greater tumor burden are considered factors that result in poorer prognoses.

Table 2 Comparison of MRI findings between progression and nonprogression groups

Characteristics	Progression ($n = 44$)	Nonprogression ($n = 21$)	*P*-value
Size of the largest tumor on baseline MRI (mm)[a]	22.3 ± 20.8	7.8 ± 6.3	<0.001
Tumor signal intensity on MRI			
Precontrast T1WI			0.046
Hyper- or isointensity	36 (81.8)	21 (100)	
Hypointensity	8 (18.2)	0 (0)	
T2WI			<0.001
Hypo- or isointensity	11 (25.0)	20 (95.2)	
Mild to moderate hyperintensity	33 (75.0)	1 (4.8)	
Subtraction arterial phase			0.001
Isointensity	15 (34.1)	17 (81.0)	
Hyperintensity	29 (65.9)	4 (19.0)	
Hepatobiliary phase			<0.001
Hyper- or isointensity	7 (15.9)	16 (76.2)	
Hypointensity	37 (84.1)	5 (23.8)	
Diffusion restriction			<0.001
Absence	8 (18.2)	18 (85.7)	
Presence	36 (81.8)	3 (14.3)	

Unless otherwise stated, data are numbers of lesions with percentages.
MRI, magnetic resonance imaging; T1WI, T1-weighted image; T2WI, T2-weighted image.
[a]Data are mean ± SD.

Hepatic metastases from uveal melanoma typically exhibit high signal intensity on T1WI, which is attributed to shortened T1 and T2 relaxation times caused by melanin content or intratumoral hemorrhages [16–18]. The prevalence of T1 hyperintensity in hepatic metastases from uveal melanoma varies widely, with estimated ranges of 19–73% [9,19,20]. In this study, 81.8% of patients displayed T1 hyper- or isointensity. According to Balasubramanya *et al.* [9], hepatic metastases with T1 hyperintensity are indicative of well differentiated and less aggressive tumors, whereas T1 hypointensity is associated with more rapidly growing and aggressive lesions. Our findings align with these observations, as T1 hypointensity of the tumor was a significant predictor of shorter TTP. However, some studies have proposed that pronounced pigmentation in primary uveal melanomas or hepatic metastases, observed as T1 hyperintensity on MRI, may be linked to poorer prognoses [21,22]. This hypothesis remains controversial and requires further investigation.

Lee *et al.* [11] found that metastatic melanoma in the liver, regardless of its origin, tended to progress more rapidly when it exhibited intermediate high signal intensity on T2WI compared to lesions with low to iso signal intensity. Similarly, our study demonstrated that hepatic metastases from uveal melanoma with mild to moderate T2 hyperintensity were associated with a shorter TTP, the highest HR, and the highest point in the nomogram. We hypothesized that this correlation may be due to the higher signal intensity on T2WI, reflecting increased cellular water content, whereas decreased T2WI signal intensity could reflect an old hemorrhage, indicating a more chronic and stable lesion [23].

The use of hepatocyte-specific gadolinium-based contrast agents has significantly enhanced the sensitivity

Table 3 MRI findings associated with time to progression of hepatic metastases from uveal melanoma

	Univariable analysis			Multivariable analysis		
Characteristics	Hazard ratio	95% CI	*P*-value	Hazard ratio	95% CI	*P*-value
Size of the largest tumor on baseline MRI (mm)	1.051	1.032–1.070	<0.001	1.028	1.008–1.048	0.005
Tumor signal intensity on MRI						
Precontrast T1WI						
Hyper- or isointensity	–	–	–	–	–	–
Hypointensity	6.433	2.760–14.995	<0.001	3.033	1.235–7.450	0.016
T2WI						
Hypo- or isointensity	–	–	–	–	–	–
Mild to moderate hyperintensity	7.660	3.761–15.60	<0.001	3.680	1.645–8.186	0.001
Subtraction arterial phase						
Isointensity	–	–	–			
Hyperintensity	4.117	2.131–7.952	<0.001			
Hepatobiliary phase						
Hyper- or isointensity	–	–	–	–	–	–
Hypointensity	7.875	3.234–19.176	<0.001	3.370	1.208–9.400	0.020
Diffusion restriction						
Absence	–	–	–			
Presence	8.469	3.767–19.039	<0.001			

CI, confidence interval; MRI, magnetic resonance imaging; T1WI, T1-weighted image; T2WI, T2-weighted image.

Fig. 2

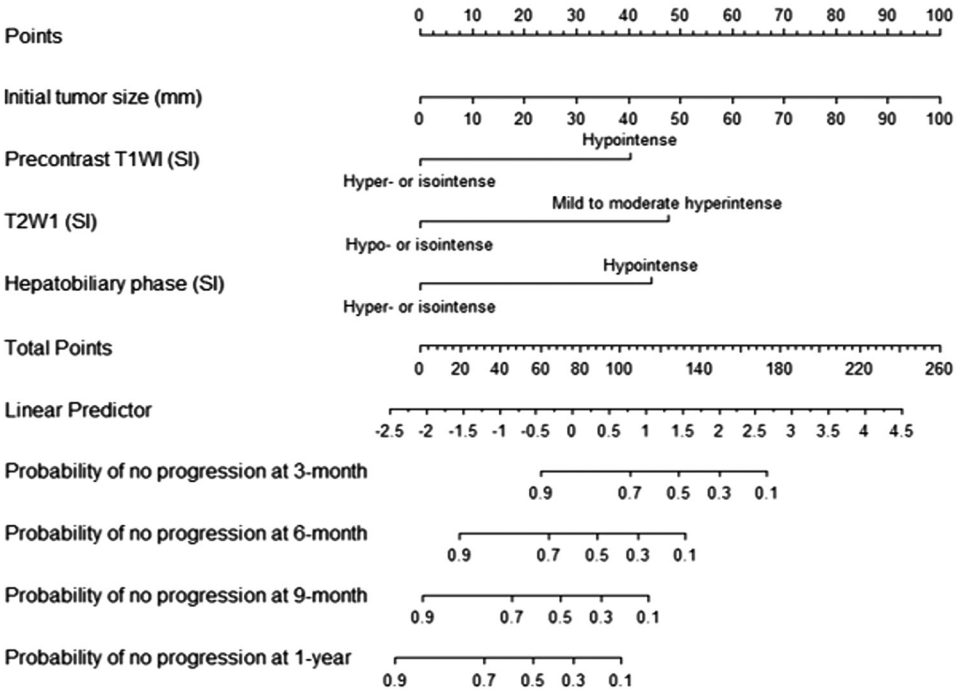

Nomogram based on gadoxetic acid-enhanced MRI for predicting the time to progression in patients with hepatic metastases of uveal melanoma. The points for each variable are found on the uppermost "points" scale. On the bottom scale, the points for all variables are added up into 'total points' and translated into probability of no tumor progression at 3, 6, and 9 months and 1 year after the baseline MRI. MRI, magnetic resonance imaging.

Fig. 3

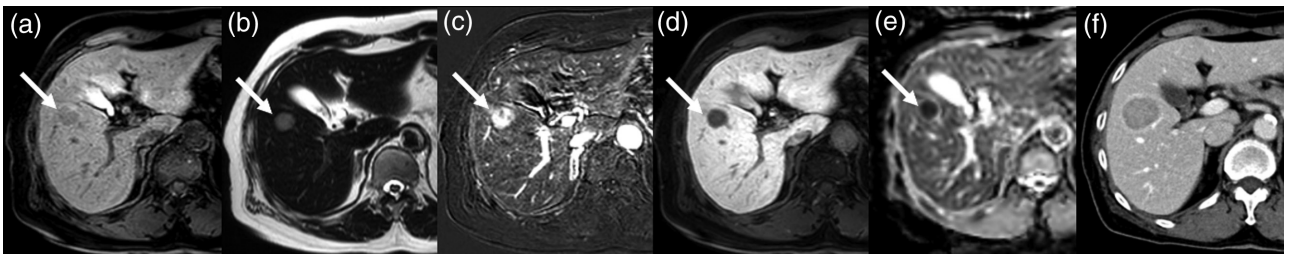

Axial MRI of a 74-year-old female with hepatic metastasis from uveal melanoma. A 20-mm tumor (arrows) showed hypointensity on precontrast T1-weighted image (a), mild to moderate hyperintensity on T2-weighted image (b), hyperintensity on subtraction arterial phase image (c), hypointensity on hepatobiliary phase image (d), and the presence of diffusion restriction on the apparent diffusion coefficient map (e). Based on the nomogram, the patient had a total of 152 points, and the probability of no tumor progression at 3 months was only 30%. On follow-up axial contrast-enhanced abdominal computed tomography (CT) on portal venous phase after 93 days (f), the tumor had grown to 39 mm, indicating progression. MRI, magnetic resonance imaging.

and specificity of MRI for detecting hepatic metastases [24], as metastatic lesions lacking hepatocytes do not display uptake of the contrast agent, causing them to appear hypointense relative to the surrounding normal liver parenchyma [9,25]. However, in our study, 35.4% of the hepatic metastases from uveal melanoma exhibited hyper- or isointensity on hepatobiliary phase, while those with hepatobiliary phase hypointensity had significantly shorter TTPs. Radiologists should be aware that hepatic metastases from uveal melanoma may appear hyper- or isointense on hepatobiliary phase, unlike other types of metastases, and may have favorable prognosis compared to hypointense lesions.

Hepatic metastases from uveal melanoma tend to demonstrate strong contrast enhancement, owing to

Fig. 4

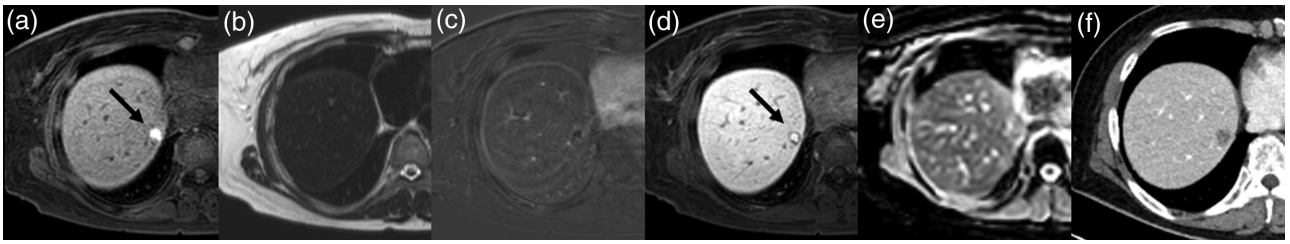

Axial MRI of a 76-year-old female with hepatic metastasis from uveal melanoma. An 11-mm tumor (arrows) showed hyperintensity on precontrast T1-weighted image (a), isointensity on T2-weighted image (b), isointensity on subtraction arterial phase image (c), hyperintensity on hepatobiliary phase image (d), and the absence of diffusion restriction on the apparent diffusion coefficient map (e). Based on the nomogram, the patient had a total of 11 points, and the probability of no tumor progression at 1 year was approximately 80%. On follow-up axial contrast-enhanced abdominal CT on portal venous phase after 361 days (f), the tumor measured to 12 mm, indicating nonprogression. MRI, magnetic resonance imaging.

their hypervascular nature [9,26]. However, the inherently high T1 signal intensity on precontrast images can obscure this enhancement, making subtraction techniques useful. Lee *et al*. [11] reported that hepatic metastases from malignant melanoma on contrast-enhanced subtraction images were associated with an increased risk of tumor progression. Duran *et al*. [20] utilized volumetric tumor enhancement as a biomarker to predict survival in patients with uveal melanoma after their first TACE. In our study, although hepatic metastases in the progression group more frequently showed arterial enhancement on subtraction images, this variable was not a significant predictor of TTP. This may be attributed to difficulties in accurately evaluating contrast enhancement on subtraction arterial phase images, as indicated by the moderate interobserver agreement, which contrasted with the good or excellent agreement observed for the other imaging variables.

This study had some limitations. First, owing to the retrospective design of the study, selection bias was inevitable. Second, we were unable to obtain pathological confirmation of hepatic metastases from uveal melanoma. Third, there was no consensus regarding the optimal treatment method for hepatic metastases from uveal melanoma, resulting in varied treatments among patients. In addition, the study cohort was collected over a relatively long-time span (2010–2023), during which treatment strategies and available therapeutic options evolved substantially. Such heterogeneity in treatment approaches may limit the applicability of our findings to contemporary clinical practice. Fourth, due to the lack of genomic analysis results from most of the primary tumor pathological samples, these data could not be included in our evaluation. Lastly, the proposed nomogram was developed using a small retrospective cohort and was not validated in an independent external population. External validation is essential to confirm the generalizability, reproducibility, and clinical utility of the model. Therefore, further validation through prospective studies with larger cohorts and external validation is needed to confirm the utility and reliability of our nomogram.

In conclusion, nomogram based on baseline gadoxetic acid-enhanced liver MRI findings can assist in estimating TTP in patients with hepatic metastases from uveal melanoma. Specifically, the significant predictors of TTP include the size of the largest tumor, precontrast T1 hypointensity, mild to moderate T2 hyperintensity, and hepatobiliary phase hypointensity of the tumor. Recognizing these features may have important implications for the prediction of the progression of hepatic metastases in patients with uveal melanoma.

Acknowledgements

This work was supported by the Soonchunhyang University Bucheon Hospital Hyangseol Research Fund (2025), National Research Foundation of Korea (NRF) grant funded by the Korea government (MSIT) (RS-2025-23963109), and the Basic Science Research Program through the NRF funded by the Ministry of Education (RS-2023-00244520). The funders had no role in the study design, data collection and analysis, decision to publish, or preparation of the manuscript.

Conflicts of interest

There are no conflicts of interest.

References

1 Singh AD, Turell ME, Topham AK. Uveal melanoma: trends in incidence, treatment, and survival. *Ophthalmology* 2011; **118**:1881–1885.
2 Strashilov S, Yordanov A. Aetiology and pathogenesis of cutaneous melanoma: current concepts and advances. *Int J Mol Sci* 2021; **22**:6395.
3 McLaughlin CC, Wu XC, Jemal A, Martin HJ, Roche LM, Chen VW. Incidence of noncutaneous melanomas in the U.S. *Cancer* 2005; **103**:1000–1007.
4 Van Raamsdonk CD, Griewank KG, Crosby MB, Garrido MC, Vemula S, Wiesner T, *et al*. Mutations in GNA11 in uveal melanoma. *N Engl J Med* 2010; **363**:2191–2199.
5 Smit KN, Jager MJ, de Klein A, Kiliç E. Uveal melanoma: towards a molecular understanding. *Prog Retin Eye Res* 2020; **75**:100800.
6 Damato B. Ocular treatment of choroidal melanoma in relation to the prevention of metastatic death – A personal view. *Prog Retin Eye Res* 2018; **66**:187–199.

7 Wu SN, Qin DY, Zhu L, Guo SJ, Li X, Huang CH, *et al*. Uveal melanoma distant metastasis prediction system: a retrospective observational study based on machine learning. *Cancer Sci* 2024; **115**:3107–3126.
8 Chattopadhyay C, Kim DW, Gombos DS, Oba J, Qin Y, Williams MD, *et al*. Uveal melanoma: from diagnosis to treatment and the science in between. *Cancer* 2016; **122**:2299–2312.
9 Balasubramanya R, Selvarajan SK, Cox M, Joshi G, Deshmukh S, Mitchell DG, O'Kane P. Imaging of ocular melanoma metastasis. *Br J Radiol* 2016; **89**:20160092.
10 Francis JH, Catalanotti F, Landa J, Barker CA, Shoushtari AN, Abramson DH. Hepatic abnormalities identified by staging MRI and accuracy of MRI of patients with uveal melanoma. *Br J Ophthalmol* 2019; **103**:1266–1271.
11 Lee M, Baek SE, Moon J, Roh YH, Lim JS, Park MS, *et al*. Dynamic contrast-enhanced MRI coupled with a subtraction technique is useful for treatment response evaluation of malignant melanoma hepatic metastasis. *Oncotarget* 2016; **7**:38513–38522.
12 Mariani P, Dureau S, Savignoni A, Rouic LL, Levy-Gabriel C, Piperno-Neumann S, *et al*. Development of a prognostic nomogram for liver metastasis of uveal melanoma patients selected by liver MRI. *Cancers (Basel)* 2019; **11**:863.
13 Eisenhauer EA, Therasse P, Bogaerts J, Schwartz LH, Sargent D, Ford R, *et al*. New response evaluation criteria in solid tumours: revised RECIST guideline (version 1.1). *Eur J Cancer* 2009; **45**:228–247.
14 Kath R, Hayungs J, Bornfeld N, Sauerwein W, Höffken K, Seeber S. Prognosis and treatment of disseminated uveal melanoma. *Cancer* 1993; **72**:2219–2223.
15 Gragoudas ES, Egan KM, Seddon JM, Glynn RJ, Walsh SM, Finn SM, *et al*. Survival of patients with metastases from uveal melanoma. *Ophthalmology* 1991; **98**:383–9; discussion 390.
16 Maniam S, Szklaruk J. Magnetic resonance imaging: review of imaging techniques and overview of liver imaging. *World J Radiol* 2010; **2**:309–322.
17 Kelekis NL, Semelka RC, Woosley JT. Malignant lesions of the liver with high signal intensity on T1-weighted MR images. *J Magn Reson Imaging* 1996; **6**:291–294.
18 Premkumar A, Marincola F, Taubenberger J, Chow C, Venzon D, Schwartzentruber D. Metastatic melanoma: correlation of MRI characteristics and histopathology. *J Magn Reson Imaging* 1996; **6**:190–194.
19 Wagner M, Mariani P, Bidard FC, Rodrigues MJ, Farkhondeh F, Cassoux N, *et al*. Diffusion-weighted MRI for uveal melanoma liver metastasis detection. *Eur Radiol* 2015; **25**:2263–2273.
20 Duran R, Chapiro J, Frangakis C, Lin M, Schlachter TR, Schernthaner RE, *et al*. Uveal melanoma metastatic to the liver: the role of quantitative volumetric contrast-enhanced mr imaging in the assessment of early tumor response after transarterial chemoembolization. *Transl Oncol* 2014; **7**:447–455.
21 Foti PV, Travali M, Farina R, Palmucci S, Spatola C, Raffaele L, *et al*. Diagnostic methods and therapeutic options of uveal melanoma with emphasis on MR imaging-Part I: MR imaging with pathologic correlation and technical considerations. *Insights Imaging* 2021; **12**:66.
22 Ramtohul T, Ait Rais K, Gardrat S, Barnhill R, Román-Román S, Cassoux N, *et al*. Prognostic implications of MRI melanin quantification and cytogenetic abnormalities in liver metastases of uveal melanoma. *Cancers (Basel)* 2021; **13**:2728.
23 Curvo-Semedo L, Brito JB, Seco MF, Costa JF, Marques CB, Caseiro-Alves F. The hypointense liver lesion on T2-weighted MR images and what it means. *Radiographics* 2010; **30**:e38.
24 Maino C, Vernuccio F, Cannella R, Cortese F, Franco PN, Gaetani C, *et al*. Liver metastases: the role of magnetic resonance imaging. *World J Gastroenterol* 2023; **29**:5180–5197.
25 Koh DM. Liver-specific contrast agents. *Cancer Imaging* 2012; **12**:363–364.
26 Bellerive C, Ouellet E, Kamaya A, Singh AD. Liver imaging techniques: recognition of uveal melanoma metastases. *Ocul Oncol Pathol* 2018; **4**:254–260.